Mapping saltmarsh vertical distribution communities in southern Portugal using high spatiotemporal resolution satellite imagery

Márcio Martins (mfcmartins@ualg.pt; https://orcid.org/0000-0002-6969-2215), Filipe Parreira (fbparreira@ualg.pt; https://orcid.org/0000-0002-6898-4742), Paula Ito (pakemi.ito@gmail.com), Simon von Sachsen-Coburg und Gotha (simon.coburg@gmail.com, https://orcid.org/0000-0001-8601-9201), Rui Santos (rosantos@ualg.pt; https://orcid.org/0000-0002-7861-4366), Carmen B. de los Santos (cbsantos@ualg.pt; https://orcid.org/0000-0002-7013-494X)

[1]Centre of Marine Sciences (CCMAR/CIMAR LA), Campus de Gambelas, Universidade do Algarve, 8005-139 Faro, Portugal

Corresponding author: Márcio Martins (mfcmartins@ualg.pt)

Address: University of Algarve, Gambelas, 8005-139 Faro Portugal

Abstract

Saltmarshes, transitional coastal habitats between terrestrial and marine ecosystems, offer crucial ecological benefits, including coastal protection, biodiversity enhancement, water purification and carbon sequestration. However, saltmarsh areas are shrinking, primarily due to human activities. Traditional monitoring approaches for saltmarsh coverage are often costly and restricted in spatial scope, prompting a shift toward remote sensing techniques. While remote sensing has proven effective for studies that cover large spatial areas, its application for smaller areas remains challenging. In this study, we trained classification models to identify saltmarsh vegetation communities in southern Portugal. We utilized high-resolution (3-meter) and high-frequency (near-daily) imagery to optimize image selection according to tidal conditions at the time of capture and developed an elevation proxy for the intertidal zone. Our model achieved an overall accuracy of 67%, estimating a total of 4,572 hectares of saltmarsh in southern Portugal, 85% located in the Ria Formosa lagoon. The middle saltmarsh zone, dominated by *Atriplex portulacoides*, *Salicornia perennis*, and *Salicornia fruticosa*, covered the largest area. The approach presented here holds promise for further refinement, enabling automated, high resolution monitoring of saltmarsh communities, which is essential for conservation and management initiatives.

Funding and acknowledgements

This study received Portuguese national funds from FCT - Foundation for Science and Technology through projects UIDB/04326/2020 (https://doi.org/10.54499/UIDB/04326/2020), UIDP/04326/2020 (https://doi.org/10.54499/UIDP/04326/2020) and LA/P/0101/2020 (https://doi.org/10.54499/LA/P/0101/2020), PhD grants 2020.06996.BD (M.M., https://doi.org/10.54499/2020.06996.BD) and 2022.11198.BD (F.P.), and contract 2020.03825.CEECIND (C.B.d.l.S;

https://doi.org/10.54499/2020.03825.CEECIND/CP1597/CT0005). We also received financial support from the project “Seaforests for blue carbon - natural capital from nature-based solutions” (EEA.BG.CALL4.012.2020; PT-INNOVATION-0081) and FAM Foundation through project Blue Carbon (Grants FAM 2023/2024). We thank Planet labs for granting us access to satellite imagery through their Education and Research program.

1. Introduction

Saltmarshes are defined as coastal transition habitats between terrestrial and marine systems and are mostly found at middle and high latitudes (Mcowen et al., 2017; Worthington et al., 2024). These ecosystems are dominated by halophytic vegetation and hypersaline soils, and often comprise the majority of the vegetated area in estuaries (Visser et al., 2019). They are considered key ecosystem providers (Barbier et al., 2011), particularly for their role in coastal protection (Shepard et al., 2011), biodiversity support (Visser et al., 2019) and removal of pollutants from the water (Andrews et al., 2008; Trevathan-Tackett et al., 2015). Over several centuries, human disturbance has led to a reduction in saltmarsh coverage (Gedan et al., 2009; Murray et al., 2019). There are many drivers behind these losses. Some of them are global, such as sea level rise combined with an artificially fixed landward margin, leading to thinning saltmarsh fringes (Lovelock et al., 2015). Others act at a local scale, such as diking, land development and land-use changes which see saltmarshes repurposed for aquaculture, salt pans and animal husbandry (Gedan et al., 2009). The continuous impacts that affect worldwide saltmarsh coverage make implementing proper management and determining saltmarsh extents of utmost importance (Pétillon et al., 2023).

Saltmarsh ecosystems are dominated by plant communities which vary along a vertical elevation gradient, mostly due to differences in hydroperiod (Visser et al., 2019), although other physical and geochemical variables can affect this distribution (Armstrong et al., 1985; Eleuterius and Eleuterius, 1979). Saltmarshes typically comprise, at a minimum, two well defined zones that differ in their exposure to salinity and flooding. The low, or submergence zone, lies below the mean high-water line and is regularly inundated by tides. As a result, it is dominated by species that are highly tolerant to both prolonged flooding and elevated salinity. The high, or emergence zone, is located above the mean high-water line and is flooded only during high spring tides. This zone is dominated by spe-

cies that are tolerant of high salinities, but not floodig (Armstrong et al., 1985; Eleuterius and Eleuterius, 1979). Some saltmarsh systems also have a middle or transition zone, identified by differences in species composition between low and high zones (Visser et al., 2019).

Due to their role in shaping sedimentary coastal regions and ecological importance, saltmarsh areas have become the point of interest in studies of coastal processes and coastal management. In order to properly monitor these habitats, we require quantitative and repeatable estimates of their distribution and area extent (Pétillon et al., 2023). Traditional vegetation mapping methods require intensive field and taxonomic work, in-situ work for every mapped location, and cannot be applied across several. As such, these methods are often slow and costly, which led to the need of methods that can be applied across different time periods, varying spatial scales and handle the inherent difficulties that arise from working in coastal and intertidal environments. Remote sensing methods, particularly when combined with supervised classification models, are useful to address the limitations of traditional habitat mapping and have been successfully used for wetland monitoring (examples reviewed in Adam et al., 2010; Pham et al., 2019). Despite limitations, the field of remote sensing is rapidly evolving, with significant improvements in the quality and quantity of data available for mapping applications.

Wetland mapping using remote sensing has employed a wide range of methodological approaches. Within supervised classification frameworks, models span from traditional statistical techniques to contemporary machine learning algorithms. Among the most commonly utilized are random forests, support vector machines, gradient boosting methods, and neural networks (Blume et al., 2023; Fu et al., 2022, 2023; Jiang et al., 2021; Pham et al., 2019). Model performance is influenced by several factors, including the choice of predictor variables, dataset size, characteristics of the training data, and the selection of hyperparameters (Jung, 2018; Lumumba et al., 2024). Consequently, comparative model evaluation has become a common practice, enabling the identification of algorithms with

the highest predictive accuracy and generalization capabilities (Fu et al., 2022; Kuhn and Johnson, 2013). Previous works have shown that access to non-visible spectrum bands is important for distinguishing vegetation types (Adam et al., 2010), with hyperspectral images usually offering better performance over multi-spectral ones (Belluco et al., 2006; Kumar and Sinha, 2014). However, even more important than spectral resolution is the spatial resolution of the images. Due to steep environmental gradients, these habitats are often found in fringes or patches of small size (Pham et al., 2019). Consequently, traditional satellite sensor resolutions (10 – 30 m) have limited ability to capture smaller features as the majority of pixels capture a mixture of different saltmarsh communities. Given the saltmarsh species' strong dependence on the elevation gradient , including topographic variables may significantly improve the performance of mapping compared to relying on spectral information alone (Farris, Defne, and Ganju 2019; Fernandez-Nunez, Burningham, and Ojeda Zujar 2017; Laengner and Van Der Wal 2022; Pham et al., 2019). However, access to topographical data is often limited, which has led to attempts to derive topography from satellite imagery. While methods to derive terrain elevation from satellite imagery are well established for terrestrial habitats, and even deeper waters (Mudd, 2020; Ashphaq et al., 2021), they are often difficult or impossible to apply to coastal areas (Ashphaq, Srivastava, and Mitra 2024; Caballero and Stumpf 2023). The fact that any captured image shows a single snapshot in time of the state of the habitat is also a limitation for intertidal saltmarsh mapping, as images captured during high tide will have parts of the saltmarsh submerged, resulting in a strong attenuation of the red and near-infrared bands by the water column, two bands which are essential to study vegetation (Hestir et al., 2008; Zomer et al., 2009). This limitation can be overcome by increasing temporal resolution, which allows images to be selected based on tidal conditions, to better account for the influence of tidal variations on spectral signatures.

Recent developments in remote sensing have addressed some of these limitations, with higher spatial, spectral and temporal resolutions. Improvements in image data, image processing and modelling tools availability and flexibility have also been significant, allowing for increasingly more refined and customized analysis pipelines. In this work, we leveraged high spatial-temporal resolution satellite imagery from the PlanetScope constellation to create tidal elevation specific image composites and indices for image classification. Our goal was to create features that can be used machine learning workflow to map saltmarsh communities, allowing the models to have proxies for elevation data that is often hard to acquire, and is highly predictive of saltmarsh distribution. As case studies, we used es the four main coastal wetlands in the Algarve region, South Portugal.

2 Material and methods

2.1 Study sites

The south of Portugal region has four main wetlands, from east to west, the Guadiana estuary, the Ria Formosa lagoon, the Arade estuary, and the Alvor lagoon (Figure 1). These wetlands comprise the majority of the saltmarsh area in southern Portugal (Santos et al., 2023a), which are protected under several legal regimes. The Ria Formosa has the highest level of protection as a Natural Park. Both the Ria Formosa and the Guadiana estuary are considered Special Protection Areas under the European Natura 2000 network for their importance for bird species and are classified as Wetlands of International Importance by the Ramsar convention. It should be noted that, while the Guadiana estuary is located both on Portuguese and Spanish territory, in this work we only focused on the Portuguese margin. All four wetlands are classified as Sites of Community importance in the European Natura 2000 network.

148 Figure 1 - Location and limits of the studied wetlands in southern Portugal.

149

150 The studied wetlands experience semi-diurnal tides, with saltmarsh communities distributed along
151 the elevation gradient. The species composition is largely similar across the four systems. In gen-
152 eral, the upper intertidal is colonized by a low saltmarsh comprised mostly of *Sporobolus mari-*
153 *timus*, *Salicornia perennis*, and *Salicornia fruticosa*. In the middle marsh, the main species are *Sali-*
154 *cornia fruticosa*, *Salicornia perennis* and *Atriplex portulacoides* and the upper saltmarsh is charac-
155 terized by more bushy species, such as *Arthrocaulon macrostachyum*, *Suaeda vera* and *Limoni-*
156 *astrum monopetalum* (Almeida et al., 2014; Amaral et al., 2023; Costa et al., 1996; Lousão, 1986).

157

158 Despite their protection levels, all these wetlands have been affected by anthropogenic pressures,
159 showing varying levels of impacts and saltmarsh loss (Santos et al., 2023b and references therein).
160 In particular, large saltmarsh areas of the Arade and Guadiana estuaries were surrounded by dykes

and converted to agriculture production in the past. When the agriculture exploration stopped, these areas with limited tidal influence were again occupied by saltmarsh communities, resulting in a different species composition from natural saltmarshes (Almeida et al., 2014; Amaral et al., 2023). The Guadiana estuary shows large coverage of the invasive species *Sporobolus montevidensis* (often known as *Spartina densiflora*) (Castillo et al., 2010). In this work, we focused on the natural saltmarsh communities, excluding saltmarshes confined by dykes.

2.2 Vegetation data collection and identification of communities

Saltmarsh vegetation communities of the main four wetlands of southern Portugal were identified based on clustering of vegetation data collected during field surveys. Quadrats (1x1 m) were placed along transects perpendicular to the shoreline. The distance between quadrats varied depending on the width of the saltmarsh fringe: in narrow fringes, quadrats were placed at 1-m intervals, whereas in wider fringes, they were placed approximately 3 m apart. This approach maximized the capture of the vegetation zonation. Two surveys were done to collect vegetation data, with minor methodological differences. Transects from survey A were collected in June and July 2019, where quadrat coordinates were determined by linear interpolation between the starting and ending points of the transect, based on its distance from the transect start. For transects from survey B (collected between April 2023 and March 2024), the coordinates of individual quadrats were recorded (hand-held GPS, Garmin GPSmap 60C, with an average 2-m error). After placing the quadrat, all species found within were recorded, and the quadrat was moved along the transect. In total, 56 transects were performed with a mean of 44 quadrats per transect, for a total of 2,448 quadrat observations (Table 1, Table S1, Figure S2).

Table 1 – Number (n) of sampled transects and quadrats per study site and transect survey (Survey A: June-July 2019, Survey B: April 2023-March 2024).

Water system	Survey	Transect n	Quadrat n
Alvor	A	6	518
Alvor	B	4	39
Arade	A	3	83
Arade	B	4	26
Guadiana	A	6	237
Guadiana	B	3	54
Ria Formosa	A	30	1491

The species names followed the currently accepted nomenclature of Plants of the World Online (POWO 2024). Saltmarsh zonation was identified using hierarchical clustering on the data of species composition, using Sørensen dissimilarity as the distance measure (also known as Bray-Curtis) and Ward's D linkage clustering method (Oksanen, 2013; Singh, 2008). Clustering was done separately for each system due to some differences in species composition. To simplify the classification system, and reduce the co-existece of classes within satellite images, each cluster was assigned to one of three saltmarsh classes: low, middle and high marsh, based on field observations of the species composition along the vertical gradient. Hereafter, vegetation or saltmarsh clusters will refer to the groups created through hierarchical clustering, while vegetation or saltmarsh communities will be used to refer to the vertical zonation groups created from those clusters.

2.3 Satellite imagery and spectral features

Satellite images were acquired from PlanetScope (8 bands, ortho-rectified, surface reflectance, 3-m resolution). A composite image of the coastal systems was created by averaging images that ensured equal temporal coverage from each quarter of 2022 to account for the effects of seasonal changes in vegetation color (e.g. due to flowering). Images used in the composite were filtered for a maximum of 10% cloud cover and maximum a tidal height of 0.3 to 0.9 m (relative to EPSG:10349

- ZH Portugal Depth, henceforth referred to as HZ). Each pixel's spectral measurements were summarised by taking the 20th quantile, in order to further reduce the impact of clouds and water reflections (Blume et al., 2023). A total of 10 images were used for Alvor and Arade, 22 for Ria Formosa, and 19 for Guadiana (larger systems required more images to ensure total spatial coverage). Satellite image selection and acquisition was done using the Planet Data API (Planet Team, 2024) with a custom tidal filtering tool (Martins, 2023) that relies on data from the Portuguese Hydrographic Institute to estimate tidal elevation at time of image capture. While the time period of the images captured does not match the one of field sampling, the studied saltmarsh communities are slow growing, with changes mostly driven by environmental factors and human impacts (Karimpour et al., 2016; Newton et al., 2020). We do not expect large changes within our study system this time period. However, transects were still visually inspected and compared to Google Earth aerial imagery to look for any changes in habitats.

Two additional spectral indices were calculated to be used as predictors in the classification models or to be used in additional data preprocessing steps. The Normalized Difference Vegetation Index (NDVI) is often used to monitor vegetation health (growth and density), with high applicability in remote sensing for agriculture and vegetation mapping (Viana et al., 2019). NDVI was calculated using the composite mosaic as:

$$NDVI = (Near\text{-}Infrared - Red) / (Near\text{-}Infrared + Red).$$

The Normalized Difference Water Index (NDWI) is used to monitor water content in water bodies and soils (McFeeters, 1996). It was calculated for two different tidal ranges: low tide (tidal height below or equal to 1 m vs HZ) and high tide (tidal height equal or over 2.9 m vs HZ). These tidal ranges maximized the captured tidal range for which satellite images were available. NDWI was calculated as:

$$NDWI = (Green - Near\text{-}Infrared) / (Green + Near\text{-}Infrared)$$

2.4 Submersion time estimation and mask creation

Another feature derived from the satellite imagery was the submersion time in the studied areas, calculated as the fraction of time that a point spent under water over the year. The submersion time was computed based on the water presence in each pixel, which was assessed on a suite of satellite images from 2022. Satellite images were acquired to maximize coverage of the tidal height range for each system (Figure S1). Water masks were created for each image based on Normalized Difference Water Index (NDWI), with values above 0 classified as water. The approximate elevation (in meters, relative to HZ) of each pixel was estimated as the minimum tidal height at which it was classified as water in any of the water masks. Then, the submersion time was calculated as the fraction of time during the year of 2022 at which that pixel's estimated elevation was lower than the tidal height. The tidal height used for each system was estimated based on the nearest tidal gauge, as given by the Portuguese Hydrographic Institute and assumed to be constant within each system. To evaluate the performance of the water-line method, we examined the Pearson's correlation coefficient between the calculated submersion time and the LIDAR-derived Digital Elevation Model for the Ria Formosa lagoon from 2011 (2-m resolution, 30-cm horizontal accuracy, 10-cm vertical accuracy; Direção-Geral do Território, 2011). Because the water line method only works for intertidal areas, only pixels with an elevation between -2.5 m and 2.5 m were used for this correlation analysis.

The vegetation dataset for supervised training of the saltmarsh mapping only included observations of the target saltmarsh communities, so a mask was created to exclude the non-saltmarsh areas at each system through unsupervised methods. There were three main steps in creating this mask. Firstly, because no saltmarsh was recorded in cells with a submersion time over 50%, those cells were masked out. Secondly, the K-means clustering method was used to cluster pixels into 25 classes based on the Blue, Green, Red, Near-Infrared, NDWI at low tide, NDWI at high tide, NDVI,

longitude and latitude variables. The pixel coordinates were included to add spatial context to the clustering, allowing for neighbour pixels to be classified as more likely to be the same class, and all variables were standardized before clustering. The selection of the class number and variables was decided by manual iteration, with visual evaluation of the results through comparison with transect ground reference data and aerial imagery from Google Earth (resolution information not available; Google, 2023) and available drone images (captured with DJI Phantom 4, RGB bands, approximately 4.5-cm resolution). Clusters identified as not being saltmarsh were masked out. The third step was the use of polygons to exclude areas which were highly modified or entirely built by humans, such as saltpans and areas where water circulation was cut off by dykes. We opted to exclude these areas as the large modifications often change the species composition and other hydro-geomorphological properties (e.g. elevation gradient and water circulation) of the site to a point where our training dataset was not representative of them. Lastly, the contiguous areas of the mask raster were shrunk and then grown by one cell, to remove stand-alone pixels known as *salt and pepper* artefacts. Raster operations were done with the *terra* package v1.7 (Hijmans, 2024) and *GRASS GIS* v8.3.2 (GRASS Development Team et al., 2024).

2.5 Classification model training and performance assessment

A supervised classification model (Figure 2) was trained to predict the natural saltmarsh communities (low, middle or high) for all four study areas, with the training workflow implemented in the *Tidymodels* framework (Kuhn and Wickham, 2020). Every individual quadrat was considered an individual observation, even when co-existence of saltmarsh communities was observed within a single satellite image pixel. The vegetation dataset (Table S2) was separated into training and testing sets with an 80/20 ratio (1,937 quadrats for training, 511 quadrats for testing). The split was stratified to ensure that the three saltmarsh classes were represented in both sets and, when possible, in all systems.

A total of 7 classifiers were tested: Regularized Multinomial Regression (package *glmnet*; Friedman et al., 2010), Random Forest (package *ranger*; Wright and Ziegler, 2017), Support Vector Machines with a radial basis and polynomial kernel functions (package *kernlab*, Karatzoglou et al., 2004), K-Nearest Neighbours (package *knn*; Schliep and Hechenbichler, 2016), Multilayer Perceptron (package *nnet*; Venables and Ripley, 2002) and extreme gradient boosting decision trees (package *xgboost*; Chen et al., 2024). For predictors, we used the full range of spectral bands from the composite mosaic, NDVI from the composite mosaic, as well as NDWI at low tide and NDWI at high tide. Two predictor transformations were tested, one where predictors were normalized (z-score), and one where models were trained on the principal components that explained 98% of variability of the predictors, as determined by Principal Component Analysis. Each combination of classifier and predictor transformation was trained with two datasets: a dataset for the whole of the Algarve (includes data for all study systems) and a wetland-specific dataset (only data for one study system). No models were trained specifically for the Arade estuary due to only one saltmarsh community being observed. Model hyperparameters were tuned using grid search and k-fold cross validation (10 folds), with folds being stratified by the target class to ensure class balance was maintained. Afterwards, the classification model with the highest median kappa statistic was selected, and the hyperparameters from the best performing fold were used to train the final model using the full training dataset.

The performance of the final supervised classifier was evaluated by comparing the agreement of the predictions with the testing dataset. The overall performance of the model was evaluated through accuracy. Confusion matrices and per-class accuracies were used to assess performance for each saltmarsh community.

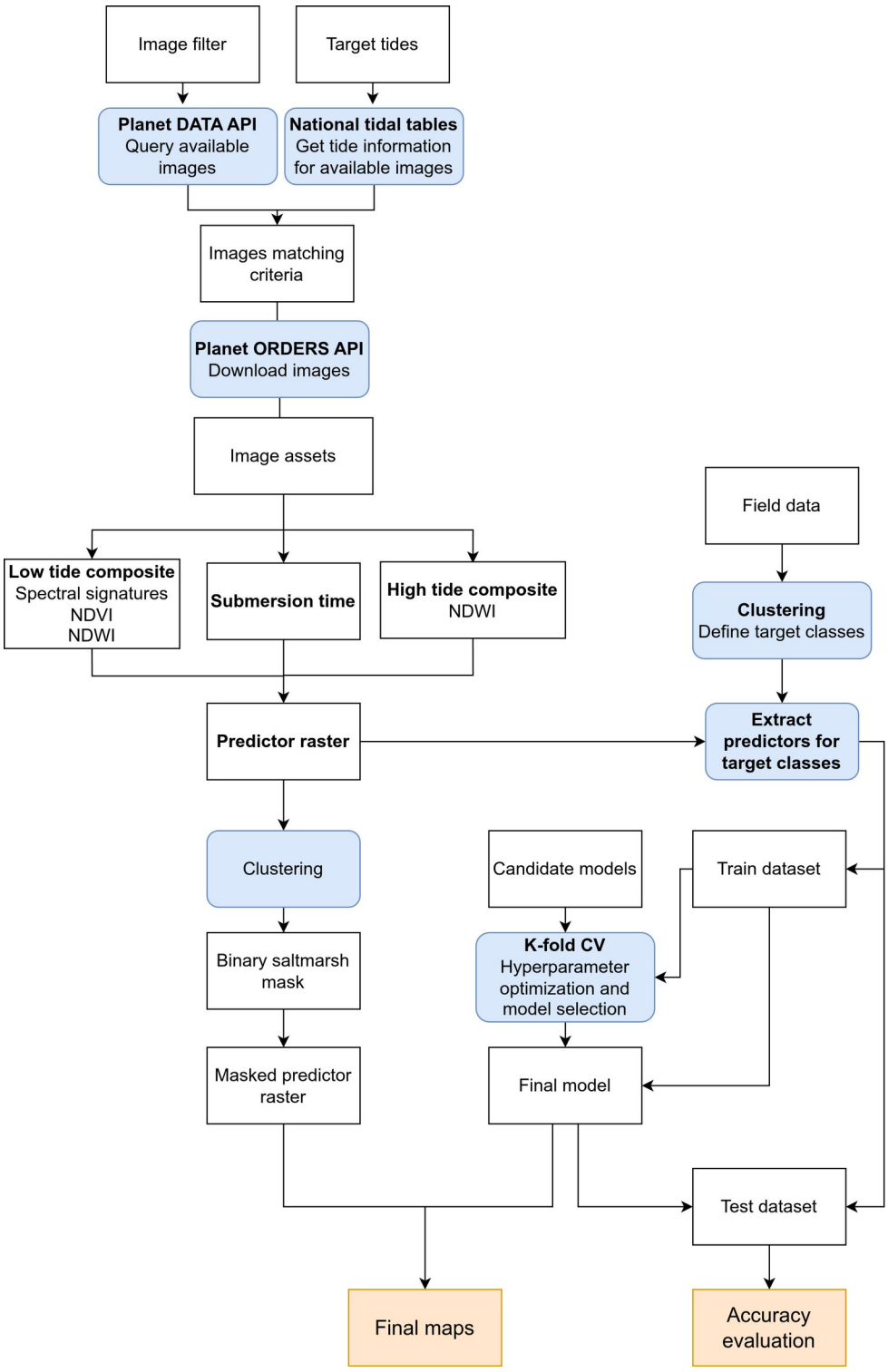

308 Figure 2 - Summary of data acquisition and classification model workflow. White boxes represent

309 data or products. Blue boxes represent processes and the orange boxes represent the final results.

3 Results

3.1 Assignment of vegetation clusters to saltmarsh communities

The number of identified vegetation clusters varied across study systems, as did the number of salt-marsh communities assigned to them (Figure 3, Table S3). In the Arade estuary, while two clusters were identified, both of them were assigned to middle saltmarsh, meaning that no other community was identified in this system. In Ria de Alvor, three clusters were identified, and each one was assigned to a unique zone. In Ria Formosa, five clusters were identified, two being assigned to low saltmarsh, two to middle saltmarsh and one to high. In Guadiana estuary, the extensive presence of the invasive species *Sporobolus montevidensis* led to a more complex cluster structure. This species can co-exist with both the low and middle saltmarsh species, making the cluster delimitation less clear. In the end, six clusters were identified and assigned to all three communities. Two of the Guadiana clusters were the result of mostly monospecific quadrats of *Sporobolus maritimus* or *Sporobolus montevidensis*.

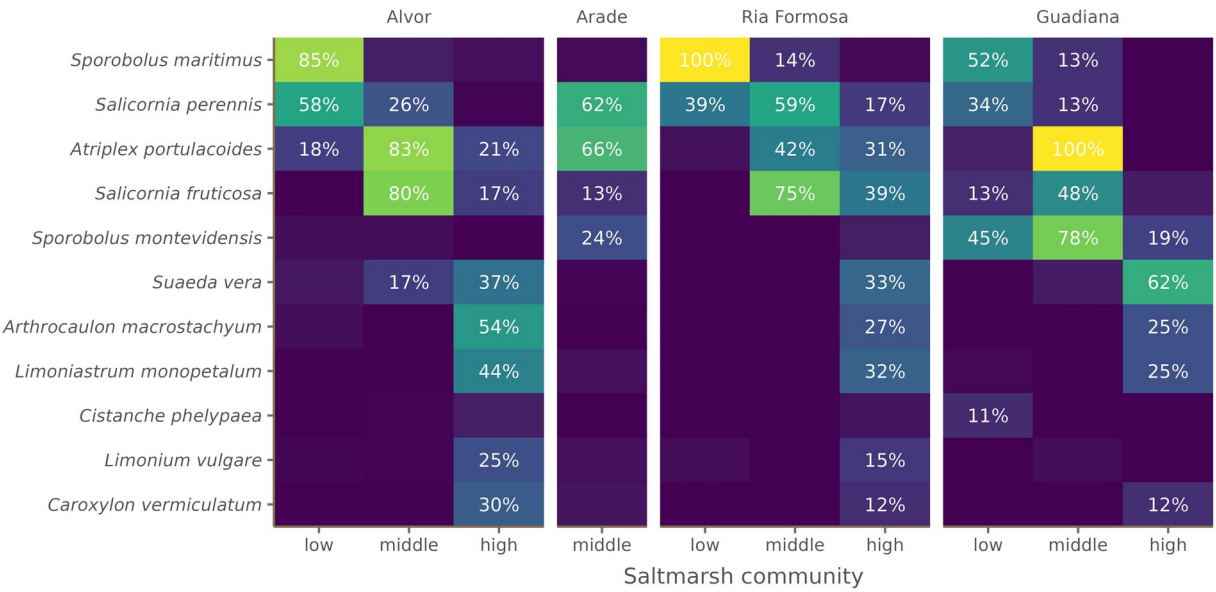

Figure 3 - Species composition of the saltmarsh communities (low, middle or high saltmarsh) for each study system. The values indicate the percentage of quadrats within a saltmarsh community in which the species was present. Species which were not observed in at least 10% of the quadrats of

any community, for any system, were excluded from this figure (but full results are available at Table S3).

Overall, for the four systems, the low saltmarsh community was dominated by *Sporobolus maritimus*, which often co-existed with *Salicornia perennis*. The most characteristic species of the middle saltmarsh were *Atriplex portulacoides*, *Salicornia perennis* and *Salicornia fruticosa*. In the Arade and Guadiana saltmarsh, we could also find the invasive species *Sporobolus montevidensis*. This species was particularly frequent in the Guadiana, where it was found in most of the middle marsh quadrats, but also in the low and high saltmarsh. High saltmarsh showed the highest number of possible species and variation across studied systems. This community showed some species overlap with the middle saltmarsh (A. *portulacoides* and *S. fruticosa*) but showed a higher presence of bushy species (*Limoniastrum monopetalum, Suaeda vera* and *Caroxylon vermiculatum),* as well as *Arthrocaulon macrostachuym* and *Limonium vulgare*.

3.2 Model features, training and selection

The estimated submersion time was significantly correlated with the LIDAR-derived elevation for the Ria Formosa, with a Pearson's correlation coefficient of -0.72 ($p < 0.001$). This relationship was particularly strong between -1 m and 1 m elevation (Figure 4). At the more extreme ends of the tidal range, the satellite-based method for submersion time showed a large dispersion in predicted values. However, the strong correlation between the submersion time feature and the elevation suggested that this is a useful proxy for elevation in systems where this information is absent.

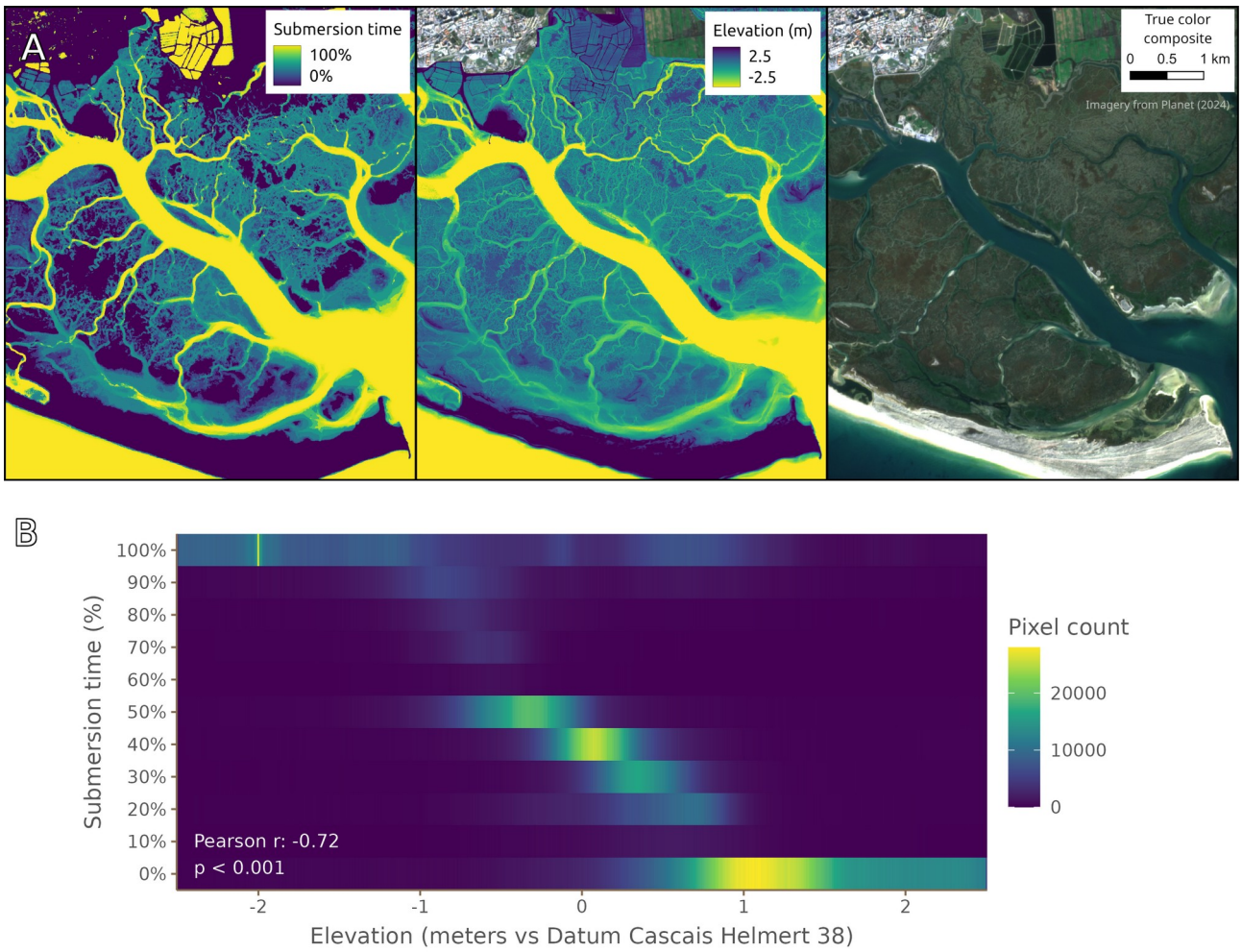

352 Figure 4 - (A) Map view comparing submersion time (left), LIDAR digital elevation model
353 (middle) and true color satellite image composite (right) for the same location in the Ria Formosa.
354 (B) Heatmap of submersion time versus elevation, with the color intensity indicating the number of
355 pixels corresponding to each pair of values. The true color satellite composite was created from
356 Planetscope imagery (Planet team, 2024). Elevation was obtained from the LIDAR DEM created by
357 Direção-Geral do Território, (2011).
358
359 Cross-validation showed similar median performances for K-Nearest Neighbours and Random
360 Forest, with normalized and principal component predictors (Figure 5). Model performance was
361 similar in the Alvor and Ria Formosa, but the fold Kappa statistic in the Guadiana showed high
362 variability, which suggests that there might be problems with the training data from that wetland.
363

For the final model, we selected the system-independent Random Forest model with normalized predictors. When evaluated on the unseen test dataset, the selected model had an overall accuracy of 67%. Prediction performance for low and middle saltmarsh were identical, with producer's accuracy of 71.1 and 73.4%, respectively (Table 2). It was lower for high saltmarsh, at only 52.5%. In terms of user accuracy (i.e. the probability of a pixel in our produced map being correct), we observed that middle saltmarsh underperformed, with a user accuracy of 58.3%, compared to the low and high saltmarsh which garnered 74.4 and 75.3%, respectively.

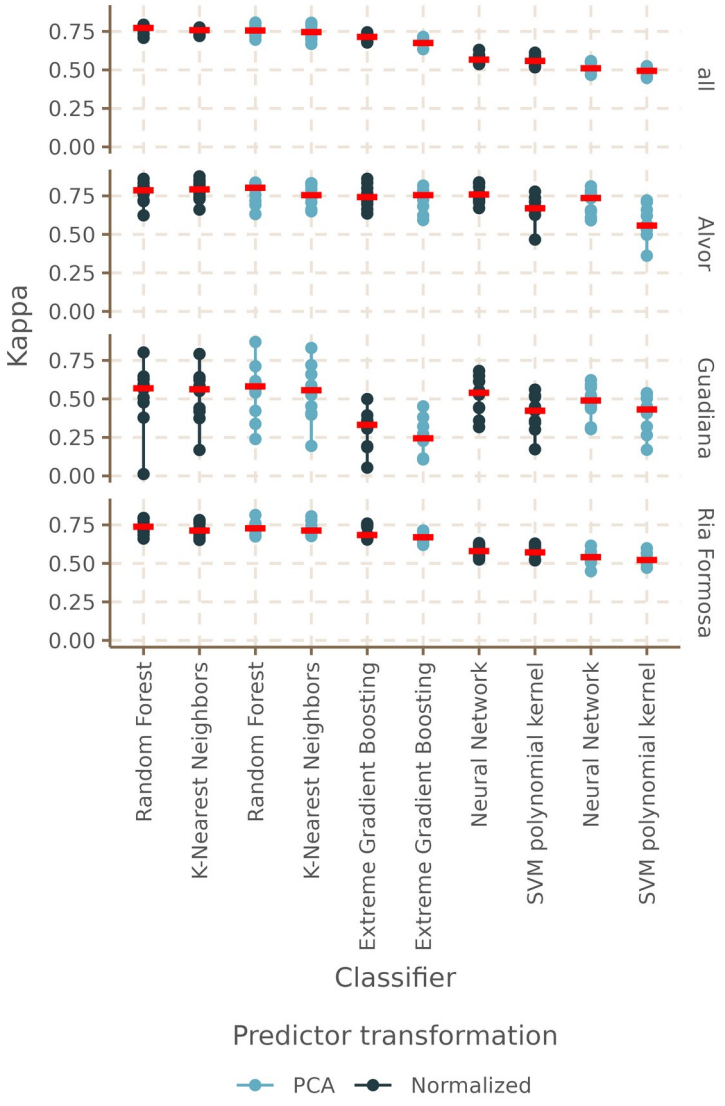

Figure 5 - Performance of the candidate classification models showed by the Kappa statistic (only the top 10 best performing candidates are shown). The panel rows separate models trained on the full vegetation dataset (all) or on data divided by study system. No models were trained for the Arade system because it contains only a single saltmarsh community.

Table 2 - Confusion matrix illustrating the performance of the classification model and accuracy statistics.

		Reference class			Total	User accuracy
		Low	Middle	High		
Predicted class	Low	128	30	14	172	74.4%
	Middle	49	141	52	242	58.3%
	High	3	21	73	97	75.3%
Total		180	192	139	511	
Producer accuracy		71.1%	73.4%	52.5%		

3.3 Saltmarsh community mapping

Using the selected model, we mapped an estimated combined total area of 4,572 ha of natural saltmarsh across the four studied wetlands, divided into 919 ha of high, 2,182 ha of middle, and 2,371 ha of low saltmarsh (Table 3). The Ria Formosa lagoon was the system with the most extensive saltmarsh area (Figure 6), with a total area of 3,897 ha, 85% of the total mapped saltmarsh in the Algarve. The second largest saltmarsh area was in the Guadiana estuary (412 ha, 9%), followed by the Arade estuary (164 ha, 4%) and lastly the Ria de Alvor (99 ha, 2%).

391 Table 3 - Estimated natural saltmarsh area for study systems, per saltmarsh community. The per-

392 centages indicate the relative frequency of that community in a system.

Community	Area (ha)			
	Alvor	**Arade**	**Ria Formosa**	**Guadiana**
Low	9 (10%)	31 (19%)	1,338 (34%)	93 (23%)
Middle	56 (56%)	116 (71%)	1,732 (45%)	278 (67%)
High	34 (34%)	17 (10%)	827 (21%)	41 (10%)
Total	**99**	**164**	**3,897**	**412**

393

394

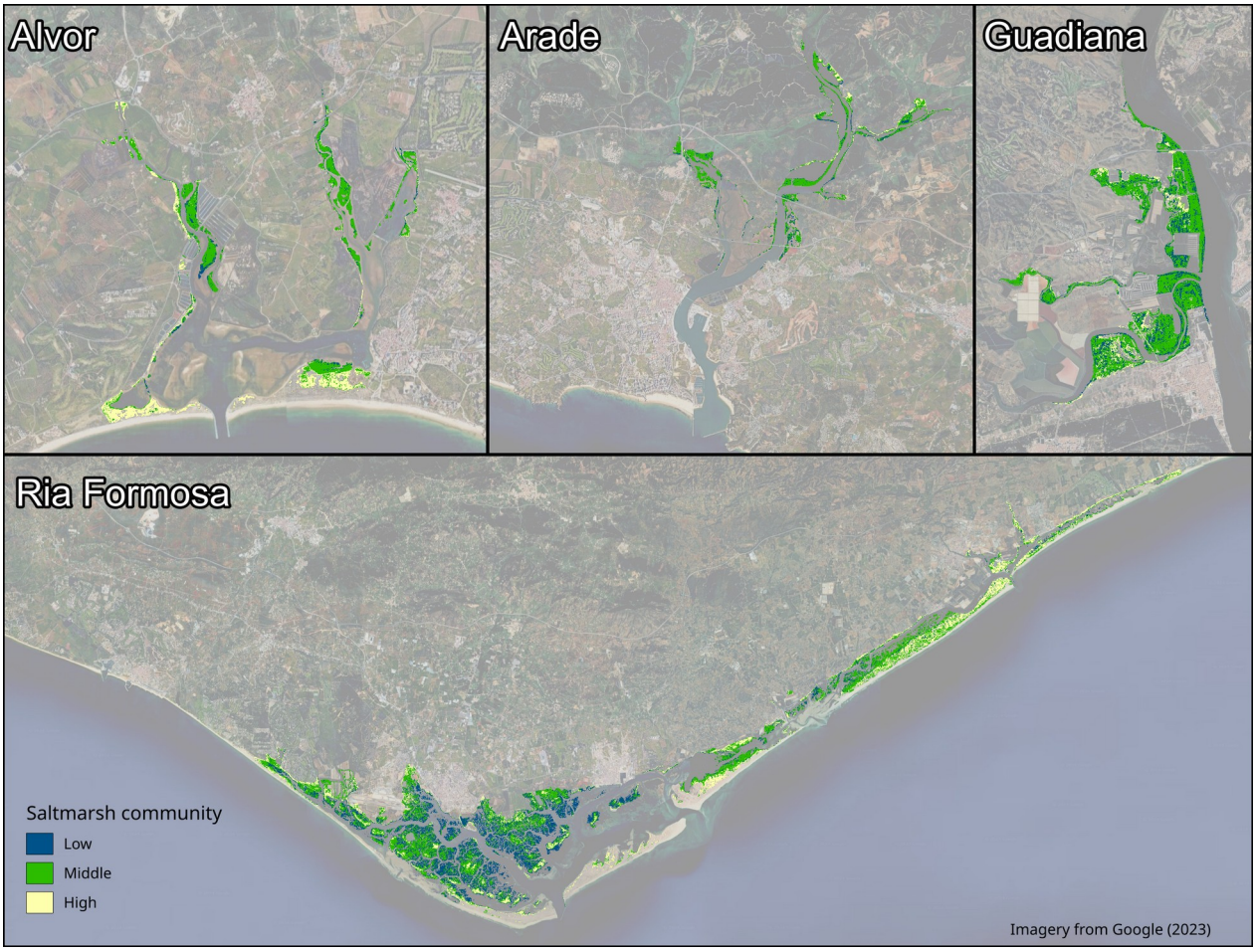

395 Figure 6 – Estimated saltmarsh distribution for studied wetlands. Prediction rasters are overlaid on a

396 desaturated satellite basemap, to increase readability.

Middle saltmarsh estimated area coverage ranged from 45 to 71%, making it the community with the highest area coverage across all systems. We found that the Arade and Guadiana estuaries did not present large areas of high saltmarsh, comprising only 10% of their total area. Ria de Alvor showed little coverage of low marsh (10%), with the highest relative area of high saltmarsh across all systems (34%). The Ria Formosa shows the most balanced distribution between saltmarsh communities.

4 Discussion

A remote sensing-based methodology capable of identifying and mapping the saltmarsh vertical distribution communities of southern Portugal was developed, which holds significant potential for refinement into a robust tool for long-term monitoring of saltmarshes in the region. The distribution and extent of the natural saltmarsh communities were quantified across the four main wetlands of the Algarve: Ria de Alvor, Arade estuary, Ria Formosa and Guadiana estuary. A total area of 4,572 ha of saltmarsh across these coastal systems was estimated. The largest natural saltmarsh area was found in the Ria Formosa lagoon, with an area approximatively 9 times that of the second-largest system, the Guadiana estuary. Among the identified communities, the middle saltmarsh dominated across all study systems (average of 48%) followed by the low saltmarsh (32%) and the high saltmarsh (20%). The middle saltmarsh was characterised primarily by the species *Salicornia perennis, Salicornia fruticosa* and *Atriplex portulacoides*, and the low saltmarsh by *Sporobulus maritimus* and *Salicornia perennis*. The high saltmarsh had a more diverse community, with more variation in species composition across wetlands, but the three main species were *Limoniuastrum monopetalum, Arthrocaulon macrostachyum* and *Suaeda vera.*

4.1. Model performance and limitations

Our study used a hybrid supervised and unsupervised workflow to map saltmarsh communities. The final supervised model achieved an overall accuracy of 67% in separating saltmarsh communities. Although this accuracy may seem modest, it is important to note that it specifically reflects the model's performance to distinguish among saltmarsh communities, rather than different habitat or land use classes. For comparison, a previous work that focused exclusively on distinguishing saltmarsh communities in a similar wetland (Cádiz Bay, southern Spain) achieved an overall accuracy of 87% (Curcio et al., 2023). These authors relied on unmanned automated vehicles, which offer the advantage of capturing images at much higher spatial resolution but are constrained by the limited spatial extent at which they can be applied. Souza and Rodrigues (2023) mapped saltmarshes in the

Ria Formosa and obtained overall accuracies from 71 to 81%. However, their analysis focused on classifying a single saltmarsh class, alongside 13 non-saltmarsh classes. Comparing methodologies with such different target classes are inherently invalid due to these fundamental differences in classification objectives. In our model, a large proportion of errors (89% of misclassified pixels) was related to the confusion between vertically adjacent saltmarsh communities. That is, a community was most often misclassified as its immediate neighbour in the vertical zonation gradient. While these are classification errors, they indicate that the model is effectively capturing the spatial distribution patterns of saltmarsh classes, as most misclassifications occur between classes with ecologically adjacent niches and that often co-occur within a single image cell. Community co-occurrence within a cell is problematic due to higher class similarity in the training data and difficulties in distinguishing them (Hossain, Jia, and Benediktsson 2016; Wang et al. 2007; Kumar and Sinha 2014), and because our method does not allow us to predict the existence of more than one community in a single cell.

In this work, we leveraged the availability of satellite imagery combined with local tidal data to optimize image selection. This approach allowed us to select images captured during low tide, maximising the visible saltmarsh area and implementing tide-dependent features as proxies for topographic data. Due to the vertical zonation of the saltmarsh communities, which is limited by the tidal regime and elevation, incorporating topographical variables is important to obtain high performance in saltmarsh classification models (Farris, Defne, and Ganju 2019; Fernandez-Nunez, Burningham, and Ojeda Zujar 2017; Laengner and Van Der Wal 2022; Pham et al., 2019). In the absence of detailed topographic data, the use of tide-dependent features can still bring improvements to current saltmarsh mapping strategies. Ideally, high-accuracy topographic data would be employed. However, these methods require expensive specialized equipment, are constrained in the timing of data acquisition by the local tidal regime (Ryu et al., 2008, Mason et al., 1995) and are limited in the spatial extent that they can cover (Curcio et al., 2024 Chadwick, 2011). The usage of satellite-derived

digital elevation models is another option. These models have been widely applied for terrestrial ecosystems (Mudd, 2020); however, traditional satellite sensors typically offer spatial resolutions in the range of tens of meters. These resolutions are unsuitable for intertidal areas where the elevation gradient is too steep, and we often found sections where the transition from supratidal to subtidal happened in less than 5 meters horizontally, areas with mud banks, and saltmarsh with high biogeomorphic complexity, because a single cell can encompass a high range of elevations. Additionally, they rely on methods which generally are incompatible with submerged, coastal or turbid areas (Ashphaq et al., 2021; Ashphaq, Srivastava, and Mitra 2024; Caballero and Stumpf 2023). The approach selected for this work is often referred to as "water-line method" and has previously been used to calculate the extent and changes in intertidal zones (Sagar et al., 2017, Ryu et al., 2008), and mudflats (Murray et al., 2012). To the best of our knowledge, this method has not yet been used to supplement supervised saltmarsh model training. This method is straightforward when accurate tidal data and high temporal frequency images are available, but the usage of a spatially constant tide elevation for the entire system is a point that can be improved for future work. Tide elevations and timing can spatially vary in a system due to bottlenecking of the water exchange with the ocean (Dias and Sousa, 2012). Another source of error could be abnormally high inputs of fresh water, but we expect the usage of multiple images to estimate submersion time to mitigate this impact.

Another limitation of our methodology resides in the spatial resolution of the available imagery. While the 3-m resolution used is a significant improvement over historically available imagery that commonly has resolutions in the tens of meters, we often observed the co-existence of target classes within a single pixel. This issue arises from the steep environmental gradient of the intertidal zone, which results in narrow saltmarsh communities parallel to the waterline, with sharp transitions between them. On the other hand, we found that the spectral resolution of the available images was adequate. The dimensionality reduction of the predictors through PCA had little effect on the model performance, suggesting high correlation, and therefore redundancy, among the spectral bands. This

484 does not mean that no improvements can be done in terms of spectral features. In particular, the us-
485 age of the red-edge band, which is lacking in the sensors used in this work, and additional vegeta-
486 tion indices has been shown to improve the performance in vegetation classification (Huete 2012;
487 Zeng et al. 2022). However, alternative vegetation indices might need to be developed to account
488 for differences in the sensors used, as not all image bands from Planet labs are equivalent to more
489 studied sensors. Despite this , we believe that enhancing the performance of saltmarsh classification
490 models is more reliant on improving spatial resolution of satellite images and obtaining topograph-
491 ical information or proxies, rather than improving spectral resolution. This conclusion is supported
492 by Blount et al. (2021), who analysed the performance of low- and high-resolution imagery to map
493 saltmarshes in the Ria Formosa wetland. They found that lower-resolution imagery tends to overes-
494 timate saltmarsh area, with errors increasing as the biogeomorphic complexity of the saltmarsh
495 fringes grows. These insights are further supported by the review of Pham et al. (2019).
496
497 The use of unsupervised methods to create a binary saltmarsh mask represents another limitation, as
498 it prevents fully automated application without user intervention. Future improvements should fo-
499 cus on transitioning this workflow fully to supervised methods, resulting in an application with min-
500 imal user input, making it more appropriate for time series analysis.
501
502 **4.2. Identification and assignment of saltmarsh communities**
503 Hierarchical clustering was effective in delimiting the most common species clusters (groups of co-
504 existing species), which follow the expected saltmarsh communities described in previous studies in
505 these wetlands (Almeida et al., 2014; Amaral et al., 2023; Costa et al., 1996; Lousão, 1986).
506
507 The species composition in the identified saltmarsh communities was consistent across the study
508 systems. The low saltmarsh was dominated by *Sporobulus maritimus* and *Salicornia perennis*,
509 which are succeeded by *Salicornia fruticosa, Atriplex portulacoides* and *Salicornia perennis* in the

middle saltmarsh. The high saltmarsh showed a much higher species diversity, with an increased number of bushy species. The species showing the greatest variability across the studied wetlands was the invasive *Sporobolus montevidensis*. This species is well established in the Guadiana and Arade estuaries, where it was found in low, middle, and high saltmarsh areas. In the Guadiana, it tends to dominate the areas that it colonizes, forming monospecific stands. *Sporobolus montevidensis* was also found in the eastern section of Ria Formosa, although with relatively low coverage. This species is highly adaptive to changes in sediment properties and capable of displacing native saltmarsh communities (Castillo et al., 2010; García et al., 1985). Its expansion poses a significant threat to autochthonous species in the region, as already observed in the Guadiana estuary. The usage of satellite-based mapping of saltmarshes is a promising tool to monitor its expansion, providing insights into changes in their distribution and supporting management efforts to control this invasive species. However, the patches of *Sporobolus montevidensis* observed in the study area were usually smaller than the spatial resolution of the satellite images we used, or it co-occurred in mixed stands with other species. In these cases, isolating the spectral signatures of this species is difficult, if not unfeasible. We believe that these issues led to the high variability in the model performance during cross-validation, and that further research is required to evaluate the feasibility of mapping *S. montevidensis* using remote sensing data in this particular site.

In this work, we opted to exclude highly anthropogenically modified saltmarshes due to the observed differences in environmental gradients and species composition compared to natural saltmarshes. Most of these modified saltmarshes are the result of reclamation of artificially flattened areas behind dykes that alter or completely isolate them from the influence of tides (Sousa et al., 2020). The combination of the altered tidal regime, distinct species composition (Almeida et al., 2014; Amaral et al., 2023) and the absence of training data for these saltmarshes reduced our confidence in the model's ability to accurately identify these saltmarsh communities. Even in some natural sites, the lack of a well-defined or even a non-existent elevation gradient resulted in saltmarsh

areas where communities form interspersed patches (Figure 7). The exclusion of the modified areas results in an underestimation of the total saltmarsh area across the study system. Accurately classifying such areas would require improvements in the water-line method to better account for the spatial variation in tidal elevation, as well as the collection of updated, site-specific vegetation data for model training and testing purposes. Incorporating such areas into new mapping efforts, could broad the model's application to monitor restoration initiatives of saltmarshes, which often target degraded modified saltmarsh habitats.

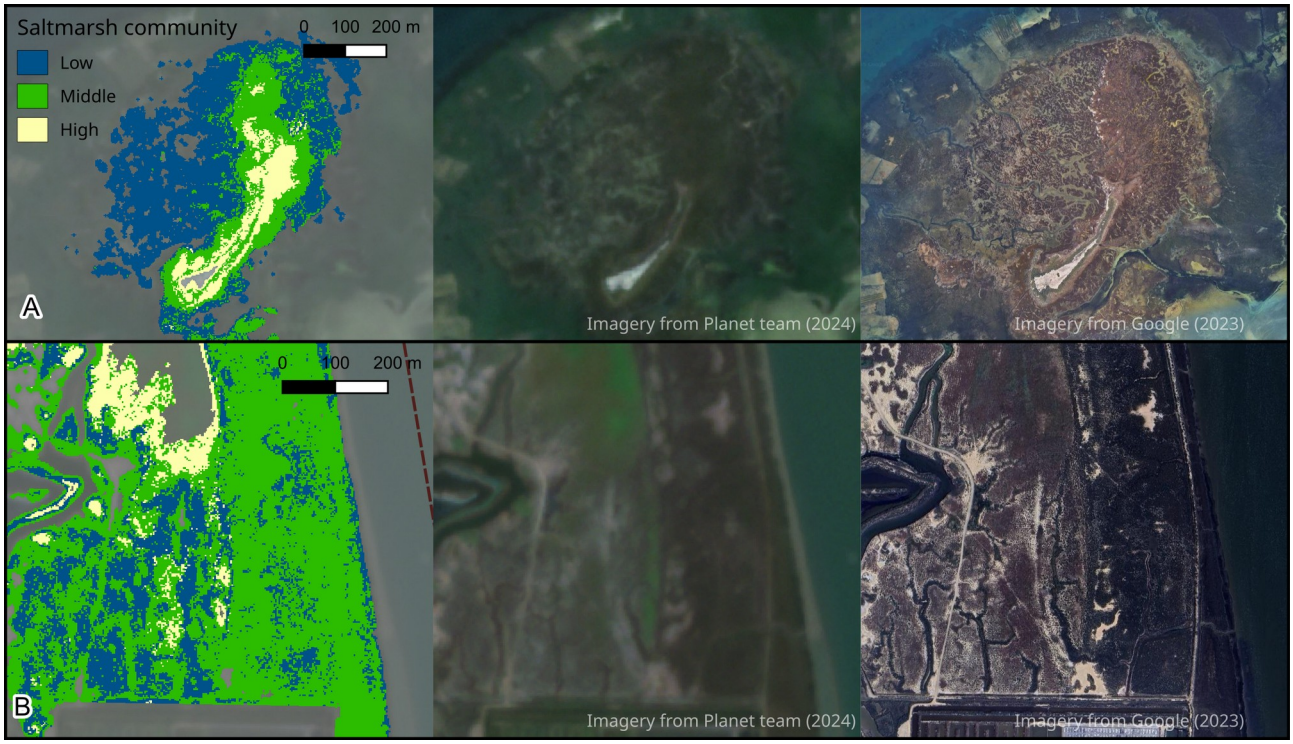

Figure 7 – Examples of the final mapping output in the Ria Formosa lagoon (left column), real colour view of the satellite image composite (middle composite; Planet team, 2024) and Google Earth imagery (right column; Google, 2023) for two sites: (A) Site with a gradual transition from low to middle and high marsh in the Ria Formosa lagoon; (B) site in the Guadiana estuary where a less accentuated vertical elevation gradient leads to large flat saltmarsh areas, with less accurate mapping results.

552 **4.3. Saltmarsh area in the Algarve**

553 We estimated that non-anthropogenically modified saltmarshes in the Algarve cover an area of ap-
554 proximately 4,572 ha. The most common saltmarsh community was the middle saltmarsh, account-
555 ing for 45 to 71% of the total saltmarsh area in each system. However, it is important to note that
556 the middle saltmarsh is also likely the most overestimated class, with a user accuracy of 58.3%.
557 This can be attributed to its nature as the transition between low to high saltmarsh, including species
558 from above and below levels, making it more prone to misclassification. The predicted saltmarsh
559 proportions were consistent with the field sampling data, where middle saltmarsh represented
560 41.5% of the in-situ observations.

561

562 The saltmarsh area estimated in this study falls within range of previous estimates (Table 4).
563 Mcowen et al. (2017) compiled the global extent of saltmarshes for 2010, categorized their estim-
564 ates based on the data quality. In the studied wetlands, two remote sensing estimates were provided:
565 one with ground-truthing validation of the estimate, and one without. In the Guadiana, our estimate
566 was 4-fold higher than the ground-truth estimate of Mcowen et al. (2017), but half of the non-valid-
567 ated one. The Guadiana estuary has vast areas of flat saltmarsh partially or totally enclosed by
568 dykes that have been modified for livestock farming, making those areas harder to identify as salt-
569 marsh. While we removed those modified saltmarshes from our analysis, Mcowen et al. (2017) in-
570 cluded them in the non-ground-truth estimate, which partially explains the large differences in the
571 saltmarsh area estimated. In Ria Formosa, the ground-truth area estimated by Mcowen et al. (2017)
572 was smaller than our estimate, with the most significant difference arising from areas that we classi-
573 fied as high saltmarsh.

574

575 Table 4 - Comparison of previous estimates for saltmarsh areas in the study systems with estimates
576 from this work. (1) Estimate for 2010 by Mcowen et al. (2017). When a range is provided, the lower

value is the ground-truthed record and highest is the full extent mapped; (2) Estimate for 2010 by Almeida et al. (2014).

	Alvor	Arade	Ria Formosa	Guadiana
References	49 ha (1) 72 ha (2)	87 ha (1) 118 ha (2)	2,978 - 6,048 ha (1)	127 - 1,067 ha (1)
Our estimate	99 ha	164 ha	3,897 ha	412 ha

4.4 Conclusions and future perspectives

Improvements of remote sensing technology have brought higher spatiotemporal resolution imagery, allowing for a higher flexibility in the methods used for coastal remote sensing. This increased flexibility makes the technology more suitable for local and regional studies, rather than being limited to large-scale applications, thereby enhancing its potential for habitat monitoring efforts.

The workflow developed in this study may be used to improve saltmarsh area estimates of coastal ecosystems, with the particular benefit of delimiting saltmarsh vertical distribution communities. This last step, which is often overlooked, is crucial for accurately assessing the delivery of certain ecosystem services, such as carbon sequestration, as different saltmarsh elevations can exhibit significantly varying sedimentation conditions (Costa et al. 1996) and carbon accumulation potential (e.g. Mazarrasa et al., 2023).

Future work would ideally extend these methods to a fully supervised workflow, allowing us to remove the need for user made decisions. Such an approach would allow for full automation of the workflow, making it better suited for applications like analysing long-term time series data.

Declaration of Interest

The authors declare that they have no conflict of interest.

CRediT author statement

Márcio Martins: Conceptualization, Investigation, Methodology, Software, Formal analysis, Data Curation, Visualisation, Writing - Original Draft. **Filipe Parreira:** Investigation, Writing - Review & Editing. **Paula Ito:** Investigation, Writing - Review & Editing. **Simon von Sachsen-Coburg und Gotha:** Investigation, Writing - Review & Editing. **Rui Santos:** Project administration, Supervision, Resources, Writing - Review & Editing, Funding acquisition. **Carmen B. de los Santos:** Conceptualization, Project administration, Supervision, Writing - Review & Editing, Funding acquisition.

Data availability

Data used is publicly available in the Zenodo repository https://zenodo.org/records/13861892. Raw and processed satellite images were not made available due to licencing. The code used during the work is publicly available at https://github.com/MarcioFCMartins/algarve-saltmarsh.

Bibliography

Adam, Elhadi, Onisimo Mutanga, and Denis Rugege. 2010. "Multispectral and Hyperspectral Remote Sensing for Identification and Mapping of Wetland Vegetation: A Review." *Wetlands Ecology and Management* 18 (3): 281–96. https://doi.org/10.1007/s11273-009-9169-z.

Almeida, Diana, Carlos Neto, Luciana S. Esteves, and José Carlos Costa. 2014. "The Impacts of Land-Use Changes on the Recovery of Saltmarshes in Portugal." *Ocean & Coastal Management* 92 (May):40–49. https://doi.org/10.1016/j.ocecoaman.2014.02.008.

Amaral, Francisco, Castelão Rodrigues, Alexandra Teodósio, Catarina Cavaco, Fernanda Silva, Miguel Silveira, and Luís Madeira. 2023. "Plano de Cogestão 2023-2025." Comissão de Cogestão da RNSCMVRSA. https://amal.pt/images/Plano_de_Cogestão_da_RNSCMVRSA_Final_Anexos_1.pdf.

Andrews, J. E., G. Samways, and G. B. Shimmield. 2008. "Historical Storage Budgets of Organic Carbon, Nutrient and Contaminant Elements in Saltmarsh Sediments: Biogeochemical Context for Managed Realignment, Humber Estuary, UK." *Science of the Total Environment* 405 (1–3): 1–13. https://doi.org/10.1016/j.scitotenv.2008.07.044.

Armstrong, W., E. J. Wright, S. Lythe, and T. J. Gaynard. 1985. "Plant Zonation and the Effects of the Spring-Neap Tidal Cycle on Soil Aeration in a Humber Salt Marsh." *The Journal of Ecology* 73 (1): 323. https://doi.org/10.2307/2259786.

638 Ashphaq, Mohammad, Pankaj K Srivastava, and D Mitra. 2021. “Review of Near-Shore Satellite
639 Derived Bathymetry: Classification and Account of Five Decades of Coastal Bathymetry Re-
640 search.” *Journal of Ocean Engineering and Science* 6 (4): 340–59.
641 https://doi.org/10.1016/j.joes.2021.02.006.
642
643 Ashphaq, Mohammad, Pankaj K. Srivastava, and D. Mitra. 2024. “Satellite-Derived Bathymetry in
644 Dynamic Coastal Geomorphological Environments Through Machine Learning Algorithms.” *Earth
645 and Space Science* 11 (7): e2024EA003554. https://doi.org/10.1029/2024EA003554.
646
647 Barbier, Edward B., Sally D. Hacker, Chris Kennedy, Evamaria W. Koch, Adrian C. Stier, and
648 Brian R. Silliman. 2011. “The Value of Estuarine and Coastal Ecosystem Services.” *Ecological
649 Monographs* 81 (2): 169–93. https://doi.org/10.1890/10-1510.1.
650
651 Belluco, E, M Camuffo, S Ferrari, L Modenese, S Silvestri, A Marani, and M Marani. 2006. “Map-
652 ping Salt-Marsh Vegetation by Multispectral and Hyperspectral Remote Sensing.” *Remote Sensing
653 of Environment* 105 (1): 54–67. https://doi.org/10.1016/j.rse.2006.06.006.
654
655 Blount, Tegan R., A. Rita Carrasco, Sónia Cristina, and Sonia Silvestri. 2021. “Exploring Open-
656 Source Multispectral Satellite Remote Sensing as a Tool to Map Long-Term Evolution of Salt
657 Marsh Shorelines.” *Estuarine, Coastal and Shelf Science*, November, 107664.
658 https://doi.org/10.1016/j.ecss.2021.107664.
659
660 Blume, Alina, Avi Putri Pertiwi, Chengfa Benjamin Lee, and Dimosthenis Traganos. 2023. “Ba-
661 hamian Seagrass Extent and Blue Carbon Accounting Using Earth Observation.” *Frontiers in Mar-
662 ine Science* 10 (February):1058460. https://doi.org/10.3389/fmars.2023.1058460.
663

Caballero, Isabel, and Richard P. Stumpf. 2023. “Confronting Turbidity, the Major Challenge for Satellite-Derived Coastal Bathymetry.” *Science of The Total Environment* 870 (April):161898. https://doi.org/10.1016/j.scitotenv.2023.161898.

Castillo, J. M., D. R. Ayres, P. Leira-Doce, J. Bailey, M. Blum, D. R. Strong, T. Luque, and E. Figueroa. 2010. “The Production of Hybrids with High Ecological Amplitude between Exotic *Spartina Densiflora* and Native *S. Maritima* in the Iberian Peninsula.” *Diversity and Distributions* 16 (4): 547–58. https://doi.org/10.1111/j.1472-4642.2010.00673.x.

Chadwick, John. 2011. “Integrated LiDAR and IKONOS Multispectral Imagery for Mapping Mangrove Distribution and Physical Properties.” *International Journal of Remote Sensing* 32 (21): 6765–81. https://doi.org/10.1080/01431161.2010.512944.

Chen, Tianqi, Tong He, Michael Benesty, Vadim Khotilovich, Yuan Tang, Hyunsu Cho, Kailong Chen, et al. 2024. “Xgboost: Extreme Gradient Boosting.” Manual. https://CRAN.R-project.org/package=xgboost.

Costa, José Carlos, Lousã Mário, and Maria Dalila Espírito-Santo. 1996. “The Vegetation of Parque Natural Da Ria Formosa (Algarve, Portugal).” *Studia Botanica*, no. 15, 69–157.

Curcio, Andrea Celeste, Luis Barbero, and Gloria Peralta. 2023. “UAV-Hyperspectral Imaging to Estimate Species Distribution in Salt Marshes: A Case Study in the Cadiz Bay (SW Spain).” *Remote Sensing* 15 (5): 1419. https://doi.org/10.3390/rs15051419.

Curcio, Andrea Celeste, Luis Barbero, and Gloria Peralta. 2024. “Enhancing Salt Marshes Monitoring: Estimating Biomass with Drone-Derived Habitat-Specific Models.” *Remote Sensing Applications: Society and Environment* 35 (August):101216. https://doi.org/10.1016/j.rsase.2024.101216.

Dias, João, and M. Sousa. 2012. "Numerical Modeling of Ria Formosa Tidal Dynamics." *Journal of Coastal Research Journal of Coastal Research SI Journal of Coastal Research SI* 56 (September):1345–49.

Direção-Geral do Território. 2011. "Modelo Digital Do Terreno (Resolução 2 m) - Zonas Costeiras de Portugal Continental - 2011." https://www.dgterritorio.gov.pt/cartografia/cartografia-topografica/modelos-digitais-do-terreno?language=en.

Eleuterius, L. N., and C. K. Eleuterius. 1979. "Tide Levels and Salt Marsh Zonation." *Bulletin of Marine Science*, no. 29, 394–400.

Farris, Amy S., Zafer Defne, and Neil K. Ganju. 2019. "Identifying Salt Marsh Shorelines from Remotely Sensed Elevation Data and Imagery." *Remote Sensing* 11 (15): 1795. https://doi.org/10.3390/rs11151795.

Fernandez-Nunez, M., H. Burningham, and J. Ojeda Zujar. 2017. "Improving Accuracy of LiDAR-Derived Digital Terrain Models for Saltmarsh Management." *Journal of Coastal Conservation* 21 (1): 209–22. https://doi.org/10.1007/s11852-016-0492-2.

Friedman, Jerome, Trevor Hastie, and Robert Tibshirani. 2010. "Regularization Paths for Generalized Linear Models via Coordinate Descent." *Journal of Statistical Software* 33 (1). https://doi.org/10.18637/jss.v033.i01.

Fu, B., Liang, Y., Lao, Z., Sun, X., Li, S., He, H., Sun, W., and Fan, D. (2023). Quantifying scattering characteristics of mangrove species from Optuna-based optimal machine learning classification

using multi-scale feature selection and SAR image time series. *International Journal of Applied Earth Observation and Geoinformation*, *122*, 103446. https://doi.org/10.1016/j.jag.2023.103446

Gedan, K. Bromberg, B.R. Silliman, and M.D. Bertness. 2009. "Centuries of Human-Driven Change in Salt Marsh Ecosystems." *Annual Review of Marine Science* 1 (1): 117–41. https://doi.org/10.1146/annurev.marine.010908.163930.

Google. 2023. "Google Earth." Google Earth. 2023. https://www.google.cn/maps/vt?lyrs=s@189&gl=cn&x={x}&y={y}&z={z}.

GRASS Development Team, Martin Landa, Markus Neteler, Markus Metz, Anna Petrášová, Vaclav Petráš, Glynn Clements, et al. 2024. "GRASS GIS." https://doi.org/10.5281/ZENODO.5176030.

Hestir, Erin L., Shruti Khanna, Margaret E. Andrew, Maria J. Santos, Joshua H. Viers, Jonathan A. Greenberg, Sepalika S. Rajapakse, and Susan L. Ustin. 2008. "Identification of Invasive Vegetation Using Hyperspectral Remote Sensing in the California Delta Ecosystem." *Remote Sensing of Environment* 112 (11): 4034–47. https://doi.org/10.1016/j.rse.2008.01.022.

Hijmans, Robert J. 2024. "Terra: Spatial Data Analysis." Manual. https://CRAN.R-project.org/package=terra.

Huete, Alfredo R. 2012. "Vegetation Indices, Remote Sensing and Forest Monitoring." *Geography Compass* 6 (9): 513–32. https://doi.org/10.1111/j.1749-8198.2012.00507.x.

Hossain, Md. Ali, Xiuping Jia, and Jon Atli Benediktsson. 2016. "One-Class Oriented Feature Selection and Classification of Heterogeneous Remote Sensing Images." *IEEE Journal of Selected*

Topics in Applied Earth Observations and Remote Sensing 9 (4): 1606–12. https://doi.org/10.1109/JSTARS.2015.2506268.

Jiang, Y., Zhang, L., Yan, M., Qi, J., Fu, T., Fan, S., and Chen, B. (2021). High-Resolution Mangrove Forests Classification with Machine Learning Using Worldview and UAV Hyperspectral Data. *Remote Sensing*, *13*(8), 1529. https://doi.org/10.3390/rs13081529

Jung, Y. (2018). Multiple predicting *K* -fold cross-validation for model selection. *Journal of Nonparametric Statistics*, *30*(1), 197–215. https://doi.org/10.1080/10485252.2017.1404598

Karatzoglou, Alexandros, Alex Smola, Kurt Hornik, and Achim Zeileis. 2004. "Kernlab - An *S4* Package for Kernel Methods in *R*." *Journal of Statistical Software* 11 (9). https://doi.org/10.18637/jss.v011.i09.

Karimpour, A., Chen, Q., and Twilley, R. R. (2016). A Field Study of How Wind Waves and Currents May Contribute to the Deterioration of Saltmarsh Fringe. *Estuaries and Coasts*, *39*(4), 935–950. https://doi.org/10.1007/s12237-015-0047-z

Kuhn, Max, and Hadley Wickham. 2020. "Tidymodels: A Collection of Packages for Modeling and Machine Learning Using Tidyverse Principles." Manual. https://www.tidymodels.org.

Kuhn, M., and Johnson, K. (2013). *Applied Predictive Modeling*. Springer New York. https://doi.org/10.1007/978-1-4614-6849-3

766 Kumar, Lalit, and Priyakant Sinha. 2014. “Mapping Salt-Marsh Land-Cover Vegetation Using
767 High-Spatial and Hyperspectral Satellite Data to Assist Wetland Inventory.” *GIScience & Remote*
768 *Sensing* 51 (5): 483–97. https://doi.org/10.1080/15481603.2014.947838.
769
770 Laengner, Marieke Liesa, and Daphne Van Der Wal. 2022. “Satellite-Derived Trends in Inundation
771 Frequency Reveal the Fate of Saltmarshes.” *Frontiers in Marine Science* 9 (July):942719.
772 https://doi.org/10.3389/fmars.2022.942719.
773
774 Lousão, M.F. 1986. “Comunidades Halofíticas Da Reserva de Castro Marim.” PhD thesis, Lisbon:
775 Universidade Técnica de Lisboa.
776
777 Lovelock, Catherine E., Donald R. Cahoon, Daniel A. Friess, Glenn R. Guntenspergen, Ken W.
778 Krauss, Ruth Reef, Kerrylee Rogers, et al. 2015. “The Vulnerability of Indo-Pacific Mangrove
779 Forests to Sea-Level Rise.” *Nature* 526 (7574): 559–63. https://doi.org/10.1038/nature15538.
780
781 Lumumba, V., Kiprotich, D., Mpaine, M., Makena, N., and Kavita, M. (2024). Comparative Ana-
782 lysis of Cross-Validation Techniques: LOOCV, K-folds Cross-Validation, and Repeated K-folds
783 Cross-Validation in Machine Learning Models. *American Journal of Theoretical and Applied Stat-*
784 *istics*, *13*(5), 127–137. https://doi.org/10.11648/j.ajtas.20241305.13
785
786 Martins, Márcio. 2023. “Portuguese Coast Planet Image Pipeline.”
787 https://github.com/MarcioFCMartins/planet_img_pipeline.
788
789 Mason, D. C., I. J. Davenport, G. J. Robinson, R. A. Flather, and B. S. McCartney. 1995. “Con-
790 struction of an Inter-tidal Digital Elevation Model by the ‘Water-Line’ Method.” *Geophysical Re-*
791 *search Letters* 22 (23): 3187–90. https://doi.org/10.1029/95GL03168.

Mazarrasa, Inés, Joao M. Neto, Tjeerd J. Bouma, Tim Grandjean, Jordi Garcia-Orellana, Pere Masqué, María Recio, Óscar Serrano, Araceli Puente, and José A. Juanes. "Drivers of Variability in Blue Carbon Stocks and Burial Rates across European Estuarine Habitats." *Science of The Total Environment* 886 (August 2023): 163957. https://doi.org/10.1016/j.scitotenv.2023.163957.

McFeeters, S. K. 1996. "The Use of the Normalized Difference Water Index (NDWI) in the Delineation of Open Water Features." *International Journal of Remote Sensing* 17 (7): 1425–32. https://doi.org/10.1080/01431169608948714.

Mcowen, Chris, Lauren Weatherdon, Jan-Willem Bochove, Emma Sullivan, Simon Blyth, Christoph Zockler, Damon Stanwell-Smith, et al. 2017. "A Global Map of Saltmarshes." *Biodiversity Data Journal* 5 (1): e11764. https://doi.org/10.3897/BDJ.5.e11764.

Mudd, Simon M. 2020. "Topographic Data from Satellites." In *Developments in Earth Surface Processes*, 23:91–128. Elsevier. https://doi.org/10.1016/B978-0-444-64177-9.00004-7.

Murray, Nicholas J, Stuart R Phinn, Michael DeWitt, Renata Ferrari, Renee Johnston, Mitchell B Lyons, Nicholas Clinton, David Thau, and Richard A Fuller. 2019. "The Global Distribution and Trajectory of Tidal Flats." *Nature* 565 (7738): 222–25. https://doi.org/10.1038/s41586-018-0805-8.

Murray, Nicholas, Stuart Phinn, Robert Clemens, Chris Roelfsema, and Richard Fuller. 2012. "Continental Scale Mapping of Tidal Flats across East Asia Using the Landsat Archive." *Remote Sensing* 4 (11): 3417–26. https://doi.org/10.3390/rs4113417.

Newton, A., Icely, J., Cristina, S., Perillo, G. M. E., Turner, R. E., Ashan, D., Cragg, S., Luo, Y., Tu, C., Li, Y., Zhang, H., Ramesh, R., Forbes, D. L., Solidoro, C., Béjaoui, B., Gao, S., Pastres, R., Kelsey, H., Taillie, D., … Kuenzer, C. (2020). Anthropogenic, Direct Pressures on Coastal Wetlands. *Frontiers in Ecology and Evolution*, *8*, 144. https://doi.org/10.3389/fevo.2020.00144

Oksanen, Jari. 2013. "Multivariate Analysis of Ecological Communities in R: Vegan Tutorial." *R Package*. https://doi.org/10.1111/j.2042-7158.1975.tb10234.x.

Pétillon, Julien, Emma McKinley, Meghan Alexander, Janine B. Adams, Christine Angelini, Thorsten Balke, John N. Griffin, et al. 2023. "Top Ten Priorities for Global Saltmarsh Restoration, Conservation and Ecosystem Service Research." *Science of The Total Environment* 898 (November):165544. https://doi.org/10.1016/j.scitotenv.2023.165544.

Pham, Tien Dat, Junshi Xia, Nam Thang Ha, Dieu Tien Bui, Nga Nhu Le, and Wataru Tekeuchi. 2019. "A Review of Remote Sensing Approaches for Monitoring Blue Carbon Ecosystems: Mangroves, Seagrasses sand Salt Marshes during 2010–2018." *Sensors* 19 (8): 1933. https://doi.org/10.3390/s19081933.

Planet Team. 2024. "Planet Application Program Interface: In Space for Life on Earth." San Francisco, CA. https://api.planet.com.

POWO. 2024. "Plants of the World Online. Facilitated by the Royal Botanic Gardens, Kew." 2024. https://powo.science.kew.org/.

Ryu, Joo-Hyung, Chang-Hwan Kim, Yoon-Kyung Lee, Joong-Sun Won, Seung-Soo Chun, and Saro Lee. 2008. "Detecting the Intertidal Morphologic Change Using Satellite Data." *Estuarine, Coastal and Shelf Science* 78 (4): 623–32. https://doi.org/10.1016/j.ecss.2008.01.020.

Sagar, Stephen, Dale Roberts, Biswajit Bala, and Leo Lymburner. 2017. "Extracting the Intertidal Extent and Topography of the Australian Coastline from a 28 Year Time Series of Landsat Observations." *Remote Sensing of Environment* 195 (June):153–69. https://doi.org/10.1016/j.rse.2017.04.009.

Santos, Rui, Paula Ito, and Carmen B. de los Santos. 2023a. "Relatório Científico I - Avaliação Dos Ecossistemas de Carbono Azul Em Portugal Continental." Scientific Report. Projeto Gulbenkian Carbono Azul. Faro: Centro de Ciências do Mar.

Santos, Rui, Paula Ito, and Carmen B. de los Santos. 2023b. "Relatório Científico II - Os 10 Principais Ecossistemas de Carbono Azul Em Portugal Continental." Scientific Report. Projeto Gulbenkian Carbono Azul. Faro: Centro de Ciências do Mar.

Schliep, Klaus, and Klaus Hechenbichler. 2016. "Kknn: Weighted k-Nearest Neighbors." Manual. https://CRAN.R-project.org/package=kknn.

Shepard, Christine C., Caitlin M. Crain, and Michael W. Beck. 2011. "The Protective Role of Coastal Marshes: A Systematic Review and Meta-Analysis." Edited by Julian Clifton. *PLoS ONE* 6 (11): e27374. https://doi.org/10.1371/journal.pone.0027374.

Singh, Warsha. 2008. "Robustness of Three Hierarchical Techniques for Ecological Data." Master's thesis, University of Iceland.

868 Sousa, Carlos A.M., Maria Emília Cunha, and Laura Ribeiro. 2020. "Tracking 130 Years of Coastal
869 Wetland Reclamation in Ria Formosa, Portugal: Opportunities for Conservation and Aquaculture."
870 *Land Use Policy* 94 (May):104544. https://doi.org/10.1016/j.landusepol.2020.104544.
871
872 Souza, Flavo Elano Soares De, and José Inácio De Jesus Rodrigues. 2023. "Evaluation of Machine
873 Learning Algorithms in the Classification of Multispectral Images from the Sentinel-2A/2B Orbital
874 Sensor for Mapping the Environmental Dynamics of Ria Formosa (Algarve, Portugal)." *ISPRS In-*
875 *ternational Journal of Geo-Information* 12 (9): 361. https://doi.org/10.3390/ijgi12090361.
876
877 Trevathan-Tackett, Stacey M., Jeffrey Kelleway, Peter I. Macreadie, John Beardall, Peter Ralph,
878 and Alecia Bellgrove. 2015. "Comparison of Marine Macrophytes for Their Contributions to Blue
879 Carbon Sequestration." *Ecology* 96 (11): 3043–57. https://doi.org/10.1890/15-0149.1.sm.
880
881 Venables, W. N., and B. D. Ripley. 2002. *Modern Applied Statistics with S*. 4th ed. New York:
882 Springer. https://www.stats.ox.ac.uk/pub/MASS4/.
883
884 Viana, Cláudia M., Sandra Oliveira, Sérgio C. Oliveira, and Jorge Rocha. 2019. "Land Use/Land
885 Cover Change Detection and Urban Sprawl Analysis." In *Spatial Modeling in GIS and R for Earth*
886 *and Environmental Sciences*, 621–51. Elsevier. https://doi.org/10.1016/B978-0-12-815226-
887 3.00029-6.
888
889 Visser, Jenneke M., Stephen Midway, Donald M. Baltz, and Charles E. Sasser. 2019. "Ecosystem
890 Structure of Tidal Saline Marshes." In *Coastal Wetlands*, 519–38. Elsevier.
891 https://doi.org/10.1016/B978-0-444-63893-9.00015-0.
892

Wang, Cheng, Massimo Menenti, Marc-Philippe Stoll, Enrica Belluco, and Marco Marani. 2007. "Mapping Mixed Vegetation Communities in Salt Marshes Using Airborne Spectral Data." *Remote Sensing of Environment* 107 (4): 559–70. https://doi.org/10.1016/j.rse.2006.10.007.

Wang, Yeqiao, Michael Traber, Bryan Milstead, and Sara Stevens. 2007. "Terrestrial and Submerged Aquatic Vegetation Mapping in Fire Island National Seashore Using High Spatial Resolution Remote Sensing Data." *Marine Geodesy* 30 (1–2): 77–95. https://doi.org/10.1080/01490410701296226.

Worthington, Thomas A., Mark Spalding, Emily Landis, Tania L. Maxwell, Alejandro Navarro, Lindsey S. Smart, and Nicholas J. Murray. 2024. "The Distribution of Global Tidal Marshes from Earth Observation Data." *Global Ecology and Biogeography* 33 (8): e13852. https://doi.org/10.1111/geb.13852.

Wright, Marvin N., and Andreas Ziegler. 2017. "Ranger: A Fast Implementation of Random Forests for High Dimensional Data in *C++* and *R*." *Journal of Statistical Software* 77 (1). https://doi.org/10.18637/jss.v077.i01.

Zeng, Yelu, Dalei Hao, Alfredo Huete, Benjamin Dechant, Joe Berry, Jing M. Chen, Joanna Joiner, et al. 2022. "Optical Vegetation Indices for Monitoring Terrestrial Ecosystems Globally." *Nature Reviews Earth & Environment* 3 (7): 477–93. https://doi.org/10.1038/s43017-022-00298-5.

Zomer, R.J., A. Trabucco, and S.L. Ustin. 2009. "Building Spectral Libraries for Wetlands Land Cover Classification and Hyperspectral Remote Sensing." *Journal of Environmental Management* 90 (7): 2170–77. https://doi.org/10.1016/j.jenvman.2007.06.028.

Supplementary material

Mapping saltmarsh vertical distribution communities in southern Portugal using high spatiotemporal resolution satellite imagery

Márcio Martins (mfcmartins@ualg.pt; https://orcid.org/0000-0002-6969-2215), Filipe Parreira (fbparreira@ualg.pt; https://orcid.org/0000-0002-6898-4742), Paula Ito (pakemi.ito@gmail.com), Simon von Sachsen-Coburg und Gotha (simon.coburg@gmail.com, https://orcid.org/0000-0001-8601-9201), Rui Santos (rosantos@ualg.pt; https://orcid.org/0000-0002-7861-4366), Carmen B. de los Santos (cbsantos@ualg.pt; https://orcid.org/0000-0002-7013-494X)

[1]Centre of Marine Sciences (CCMAR/CIMAR LA), Campus de Gambelas, Universidade do Algarve, 8005-139 Faro, Portugal

Figure S1

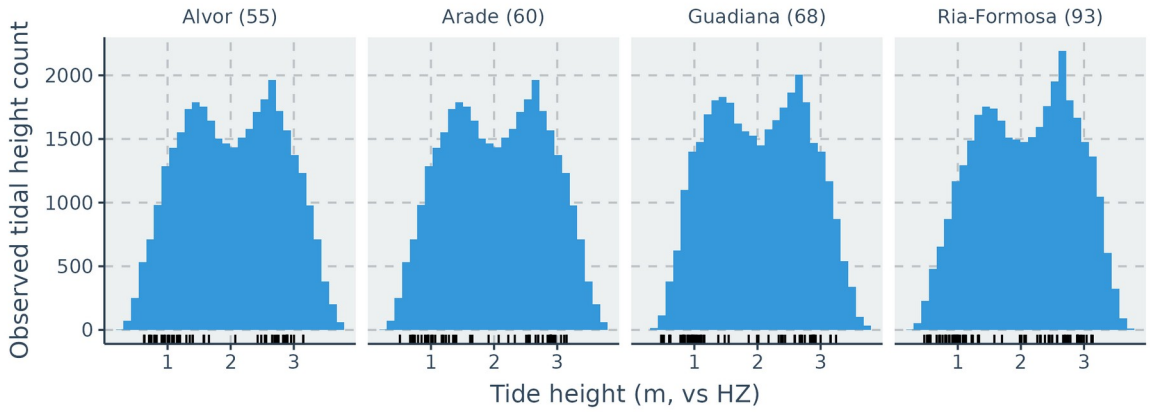

Figure S1-Distribution of tidal elevations used to create the submersion time feature for the study systems. The blue histogram shows the observed tidal elevations (m relative to EPSG: 10349 - ZH Portugal Depth), while the black lines in the X axis show elevations of the images used to estimate intertidal pixel submersion times.

Figure S2

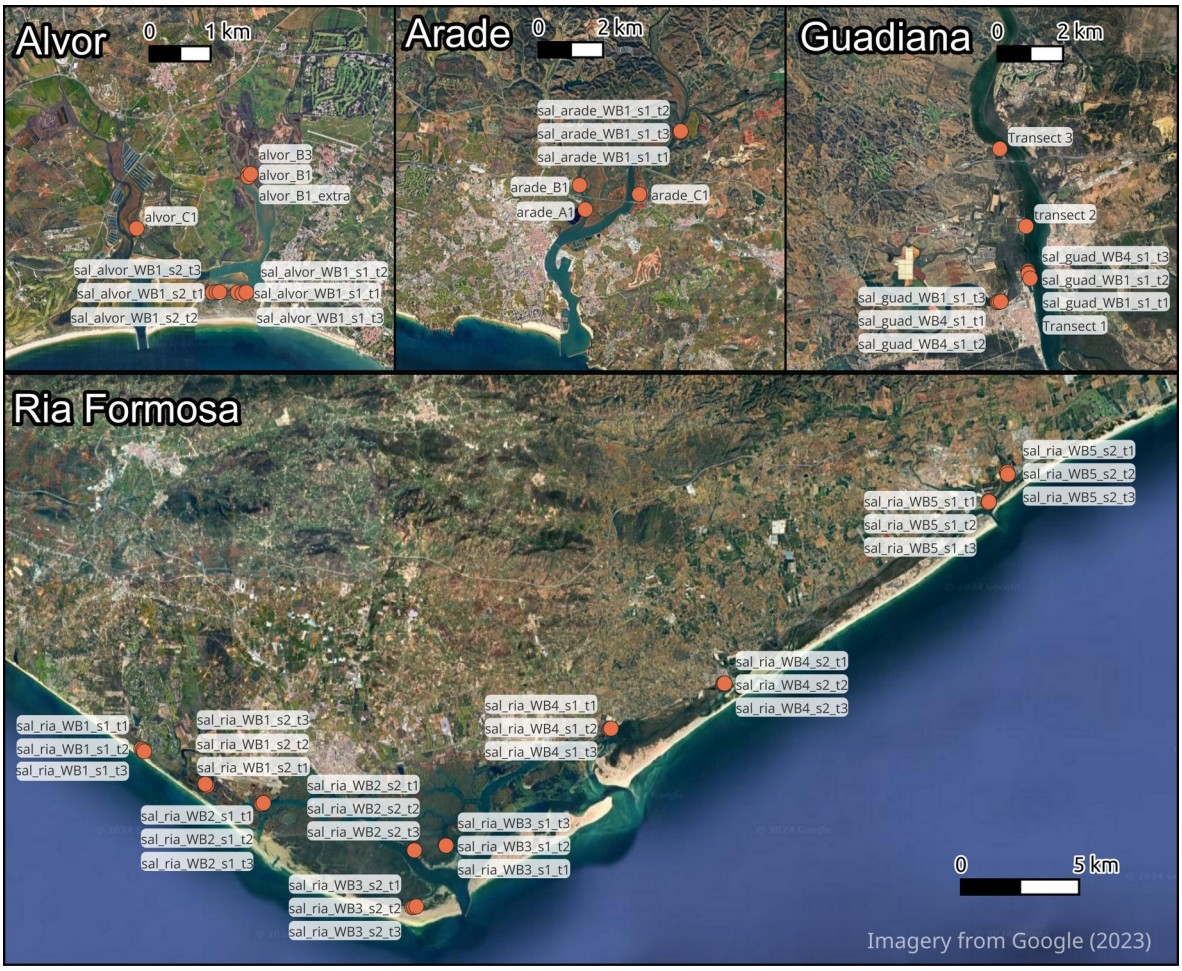

Figure S2 – Location of sampled transects for each study site.

Table S1 – Information about sampled vegetation transects. Sites are unique to each wetland.

Wetland	Survey	Site	Transect name	Date	Quadrat n
Alvor	A	1	sal_alvor_WB1_s1_t1	2019-07-19	107
Alvor	A	1	sal_alvor_WB1_s1_t2	2019-07-19	39
Alvor	A	1	sal_alvor_WB1_s1_t3	2019-07-19	49
Alvor	A	2	sal_alvor_WB1_s2_t1	2019-07-19	147
Alvor	A	2	sal_alvor_WB1_s2_t2	2019-07-19	80
Alvor	A	2	sal_alvor_WB1_s2_t3	2019-07-19	96
Arade	A	1	sal_arade_WB1_s1_t1	2019-07-18	26
Arade	A	1	sal_arade_WB1_s1_t2	2019-07-18	29
Arade	A	1	sal_arade_WB1_s1_t3	2019-07-18	28
Guadiana	A	1	sal_guad_WB1_s1_t1	2019-07-16	42
Guadiana	A	1	sal_guad_WB1_s1_t2	2019-07-16	42
Guadiana	A	1	sal_guad_WB1_s1_t3	2019-07-16	49
Guadiana	A	2	sal_guad_WB4_s1_t1	2019-07-16	34
Guadiana	A	2	sal_guad_WB4_s1_t2	2019-07-16	36
Guadiana	A	2	sal_guad_WB4_s1_t3	2019-07-16	34
Ria Formosa	A	1	sal_ria_WB1_s1_t1	2019-06-06	46
Ria Formosa	A	1	sal_ria_WB1_s1_t2	2019-06-06	47
Ria Formosa	A	1	sal_ria_WB1_s1_t3	2019-06-06	46
Ria Formosa	A	2	sal_ria_WB1_s2_t1	2019-06-06	65
Ria Formosa	A	2	sal_ria_WB1_s2_t2	2019-06-06	47
Ria Formosa	A	2	sal_ria_WB1_s2_t3	2019-06-06	43
Ria Formosa	A	3	sal_ria_WB2_s1_t1	2019-06-06	41
Ria Formosa	A	3	sal_ria_WB2_s1_t2	2019-06-06	50
Ria Formosa	A	3	sal_ria_WB2_s1_t3	2019-06-06	52
Ria Formosa	A	4	sal_ria_WB2_s2_t1	2019-06-04	40
Ria Formosa	A	4	sal_ria_WB2_s2_t2	2019-06-04	49
Ria Formosa	A	4	sal_ria_WB2_s2_t3	2019-06-04	33
Ria Formosa	A	5	sal_ria_WB3_s1_t1	2019-06-04	44
Ria Formosa	A	5	sal_ria_WB3_s1_t2	2019-06-04	43
Ria Formosa	A	5	sal_ria_WB3_s1_t3	2019-06-04	35
Ria Formosa	A	6	sal_ria_WB3_s2_t1	2019-06-03	50
Ria Formosa	A	6	sal_ria_WB3_s2_t2	2019-06-03	46
Ria Formosa	A	6	sal_ria_WB3_s2_t3	2019-06-03	50
Ria Formosa	A	7	sal_ria_WB4_s1_t1	2019-06-07	72
Ria Formosa	A	7	sal_ria_WB4_s1_t2	2019-06-07	68
Ria Formosa	A	7	sal_ria_WB4_s1_t3	2019-06-07	76
Ria Formosa	A	8	sal_ria_WB4_s2_t1	2019-06-07	47
Ria Formosa	A	8	sal_ria_WB4_s2_t2	2019-06-07	49
Ria Formosa	A	8	sal_ria_WB4_s2_t3	2019-06-07	38
Ria Formosa	A	9	sal_ria_WB5_s1_t1	2019-06-05	54
Ria Formosa	A	9	sal_ria_WB5_s1_t2	2019-06-05	82
Ria Formosa	A	9	sal_ria_WB5_s1_t3	2019-06-05	49
Ria Formosa	A	10	sal_ria_WB5_s2_t1	2019-06-05	36
Ria Formosa	A	10	sal_ria_WB5_s2_t2	2019-06-05	42
Ria Formosa	A	10	sal_ria_WB5_s2_t3	2019-06-05	51
Alvor	B	B	alvor_B1	2023-04-21	8
Alvor	B	B	alvor_B1_extra	2023-04-21	3
Alvor	B	C	alvor_C1	2023-05-09	21
Alvor	B	D	alvor_D	2023-05-09	7
Arade	B	A	arade_A1	2023-04-19	6
Arade	B	B	arade_B1	2023-04-20	2
Arade	B	C	arade_C1	2023-04-20	17
Arade	B	C	arade_C2	2023-04-20	1
Guadiana	B	A	transect 2	2023-11-14	17
Guadiana	B	B	Transect 1	2023-11-15	21
Guadiana	B	C	Transect 3	2024-03-13	16

Table S2 - Summary of train and test dataset, with number of quadrats per class and per study system.

Data set	Community	N	Study system	N
Testing	Low	180 (35.2%)	Alvor	21
			Guadiana	91
			Ria Formosa	68
	Middle	192 (37.6%)	Alvor	74
			Arade	52
			Guadiana	6
			Ria Formosa	60
	High	139 (27.2%)	Alvor	51
			Guadiana	6
			Ria Formosa	82
Training	Low	643 (33.2%)	Alvor	58
			Guadiana	138
			Ria Formosa	447
	Middle	824 (42.5%)	Alvor	262
			Arade	57
			Guadiana	40
			Ria Formosa	465
	High	470 (24.3%)	Alvor	91
			Guadiana	10
			Ria Formosa	369

Table S3 - Species composition of the saltmarsh communities (low, middle or high saltmarsh) for each study system. The values indicate the percentage of quadrats within a saltmarsh community in which the species was present.

Species	Alvor			Arade	Ria Formosa			Guadiana		
	Low	Middle	High	Middle	Low	Middle	High	Low	Middle	High
Arthrocaulon macrostachyum	2.5	0	53.5	0	0	0.2	26.8	0	0	25
Atriplex halimus	0	0	4.2	0	0	0	0	0	0	0
Atriplex portulacoides	17.7	83	21.1	66.1	2.9	41.9	30.8	8.3	100	0
Caroxylon vermiculatum	0	0	29.6	4.6	0	0	12	0	0	12.5
Cistanche phelypaea	0	0.6	7	0	0	0	4	10.9	0	0
Juncus effusus	0	0.6	0	0	0	0	0	0	0	0
Limbarda crithmoides	0	0	0	2.8	0	0	3.8	0	0	0
Limoniastrum monopetalum	0	0	43.7	2.8	0	0	31.7	1.3	0	25
Limonium vulgare	1.3	0.6	24.6	2.8	2.1	0	15.3	0	2.2	0
Myriolimon ferulaceum	0	1.2	9.2	0	0	0.2	1.8	0	0	0
Phragmites australis	0	0	0	0	0	0	1.6	0	0	0
Puccinellia maritima	0	0	0	0	0.6	0.2	4.4	0	0	0
Salicornia europaea	0	0.9	0	0	0	0.4	1.6	6.1	2.2	0
Salicornia fruticosa	0	80.4	16.9	12.8	0	75.4	39	12.7	47.8	6.2
Salicornia perennis	58.2	26.2	0.7	62.4	39.2	58.7	16.6	33.6	13	0
Spergularia bocconei	0	0	0	0	0	0.2	0	0	0	0
Sporobolus maritimus	84.8	7.4	2.8	1.8	100	13.5	1.6	52.4	13	0
Sporobolus montevidensis	2.5	2.1	0	23.9	0	0	6.7	44.5	78.3	18.8
Suaeda vera	5.1	17.3	37.3	0.9	0	0	33.5	0	6.5	62.5
Triglochin maritima	0	0	2.8	0	0	0	0	0	0	0